

Electric-field control of spin-wave power flow and caustics in thin magnetic filmsV. N. Krivoruchko,¹ A. S. Savchenko,¹ and V. V. Kruglyak²¹*Donetsk Institute for Physics and Engineering, NAS of Ukraine, 46, Nauki Avenue, 03028, Kyiv, Ukraine*²*University of Exeter, Stocker road, EX4 4QL, Exeter, Devon, United Kingdom*

(Received 26 July 2017; revised manuscript received 19 June 2018; published 26 July 2018)

An external electric field can modify the strength of the spin-orbit interaction between spins of ions in magnetic crystals. This influence leads to a spin-wave frequency shift that is linear in both the applied electric field and the wave vector of the spin wave. Here we study theoretically the external electric field as a means of control of the spin-wave power flow in thin ferromagnets. The spin-wave group velocity and focusing patterns are obtained from the slowness (isofrequency) curves by evaluating their curvature at each point of the reciprocal space. We show that the combination of the magnetodipole interaction and the electric field can result in nonreciprocal unidirectional caustic beams of dipole-exchange spin waves. We demonstrate that the degree of asymmetry of the spin-wave power flow can be tuned with the external electric field. Our findings open a novel avenue for spin-wave manipulation and development of electrically tunable magnonic devices.

DOI: [10.1103/PhysRevB.98.024427](https://doi.org/10.1103/PhysRevB.98.024427)**I. INTRODUCTION**

The possibility of an electric-field control of spin waves is well known [1–4]. If the crystal symmetry of a simple ferromagnet contains the spatial inversion element, the external electric field induces a frequency shift that is linear in both the applied electric field and the wave vector of spin wave [1–4]. In fact, this is an example of different topological effects in quantum mechanics: an extra topological phase is acquired by the quantum orbital motion of neutral magnetic moments in mesoscopic rings in the electric field. Particularly, in a ferromagnet, spin waves that propagate in the applied electric field acquire an additional quantum phase, the so-called Aharonov-Casher phase [5,6]. Microscopically this effect originates from the spin-orbit interaction. To linear order in the electric field, this effect is equivalent to adding a Dzyaloshinskii-Moriya-like (DM-like) interaction between the spins \mathbf{S}_i and \mathbf{S}_j of neighboring ions. The DM-like interaction can be presented in a traditional form as $\mathbf{d}_{ij}(\mathbf{S}_i \times \mathbf{S}_j)$, where \mathbf{d}_{ij} is a vector perpendicular to both the electric field \mathbf{E} and the unit vector \mathbf{e}_{ij} along the line that connects the magnetic ions [1–4]. The microscopic calculations [2] based on the superexchange model yield $\mathbf{d}_{ij} = Ae(\mathbf{E} \times \mathbf{e}_{ij})/E_{SO}$, where A is the Heisenberg exchange coupling, e is the absolute value of the electron charge, and E_{SO} is an energy scale associated with the inverse strength of the spin-orbit coupling. Similar to the conventional DM interaction, it is DM-like interaction results in a frequency shift that is linear in both the applied electric field and the wave vector of the spin wave.

Originally, the frequency shift was expected to be small ($\sim 0.01\%$) [6]. However, subsequent microscopic calculations based on the superexchange model pointed out that the electric-field effect could be sufficiently large to be used to control efficiently spin currents [2,3]. Furthermore, recent experimental studies showed an efficient spin-wave electrical tuning in thin magnetic films, such as YIG ($\text{Y}_3\text{Fe}_5\text{O}_{12}$) [4]. At present, interest to such phenomena is very active due to their potential applications in magnon spintronics and magnonics

[7–9], where an electrically controlled phase shifter for spin waves could become an essential component of spin-wave devices. Nonreciprocity and unidirectionality of spin-wave propagation would be also valuable for this purpose [10].

In a system with the DM interaction, the exchange spin-wave dispersion curve for propagation perpendicular to the magnetization is approximately a parabola with the frequency minimum shifted away from the origin along the wave vector axis. As a result, in some frequency regions, the spin-wave group velocity is opposite to the phase velocity, which corresponds to the case of so-called “backward” waves [11]. Additionally, as for any anisotropic medium, in a system with the DM interaction, one can create conditions when the energy transferred from a point source will flow away not as circular waves but in highly focused beams, the so-called caustics [12]. The focusing pattern can be obtained from the slowness curves (curves of constant frequency $\omega/2\pi$ in the wave vector \mathbf{k} space) by finding the normal to the slowness curve and then evaluating the curvature at each point on the curve.

Here we examine theoretically a possibility of the electric-field control of spin-wave propagation and focusing in thin magnetic films. The spin-wave focusing in a thin ferromagnetic film with conventional DM interaction was just recently examined theoretically in Ref. [13]. The authors analyzed how the slowness curves change as the film thickness is increased and the magnetodipolar interaction becomes more important. In this report, based on physics of another microscopic origin, we examine theoretically how the focusing effect can be manipulated by the external electric field keeping the film thickness constant. In particular, we demonstrate that the unidirectional dipole-exchange spin-wave caustic beams predicted in Ref. [13] to exist in systems with the DM interaction can also be formed in more conventional magnetic systems by applying an out-of-plane electric field.

In Sec. II we analyze the spin-wave dispersion and the shape of the slowness curves with and without the electric field. In Sec. III the spin-wave focusing effect and formation

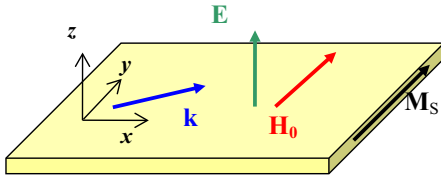


FIG. 1. Schematics of the geometry for spin-wave propagation in a tangentially magnetized film. The magnetic field \mathbf{H}_0 and the static magnetization \mathbf{M}_S are along the y direction. The electric field \mathbf{E} is orthogonal to \mathbf{M}_S .

of the electrically tunable caustics are discussed. The focusing directions are shown to be tunable with the frequency and the applied field, indicating that this effect might be useful in signal processing devices, such as tunable filters and frequency splitters. Numerical examples are presented for a thin ferromagnetic film of fixed thickness and different magnitudes of the electric field.

II. SPIN DYNAMICS IN AN ELECTRIC FIELD

Let us consider a thin (~ 10 -nm-thick) magnetic film. The film is in the x - y plane, and an in-plane magnetic field \mathbf{H}_0 is parallel to the y axis, as illustrated in Fig. 1. Notice that tangentially magnetized films are particularly convenient for the excitation and propagation of exchange spin waves [14]. We therefore concentrate on the case when the applied magnetic field is large enough so that the equilibrium magnetization \mathbf{M}_S lies in the plane of the film and $\mathbf{M}_S \parallel \mathbf{y}$. Also we consider the case of the electric field and the wave vector of spin waves being orthogonal to each other. In this geometry, the \mathbf{E} -induced phase shift of the spin waves is maximized, whereas the so-called Doppler shift due to the electric field vanishes; for more details see Ref. [15].

The theory of magnetostatic modes in homogeneous ferromagnetic films is well established (see, e.g., Refs. [16–19]), and here we give only the final equations necessary for our investigation. We focus our attention to films sufficiently thin, so that only a single spin-wave branch with amplitude uniform across the film thickness needs to be considered. Taking into account the magnetodipole and exchange interactions, the Zeeman energy associated with the applied magnetic field and the effective uniaxial (shape) anisotropy, the spin-wave frequency is

$$\omega_0(\mathbf{k}) = \gamma \mu_0 [H_x(k)H_y(k)]^{1/2}. \quad (1)$$

Here γ is the gyromagnetic ratio, μ_0 is the vacuum permeability, and

$$H_x(k) = H_0 + Dk^2 + M_S d(k_x^2/2k), \quad (2)$$

$$H_y(k) = H_0 + Dk^2 - H_K - M_S d(k/2), \quad (3)$$

where M_S is the saturation magnetization, $D = 2A/\mu_0 M_S$, where A stands for the exchange interaction constant, d is the film thickness, the wave vector \mathbf{k} is in the x - y plane, $k = (k_x^2 + k_y^2)^{1/2}$, and $H_K = (2K_u - \mu_0 M_S^2)/\mu_0 M_S$ is the effective anisotropy field, where K_u is out-of-plane anisotropy. Here we take into account that in the thin-film limit $kd \ll 1$, the dominant contribution to the dipole field is linear in k [19], and

the angle φ_k between the magnon wave vector \mathbf{k} and the y axis is $\sin \varphi_k = k_x/k$. Equation (3) shows that, in a sufficiently thin film, the dipolar energy generates in the dispersion relation a negative term linear in the wave vector. The exchange stiffness leads to a positive term quadratic in the wave vector. So, at finite wave vectors, the dispersion relation has a minimum.

The external electric field modifies the dispersion. Just as the magnetic field shifts the dispersion vertically by increasing or decreasing the frequency at fixed \mathbf{k} , the electric field shifts the dispersion horizontally by increasing or decreasing the wave vector at a fixed frequency [1–4]. For a geometry in which the wave vector ($\mathbf{k} \parallel \mathbf{x}$), the magnetization ($\mathbf{M}_S \parallel \mathbf{y}$), and the electric field ($\mathbf{E} \parallel \mathbf{z}$) are mutually orthogonal, the largest relative wave vector shift is for the lowest lying modes [3]. Following these observations, we apply the electric field normal to the x - y plane and consider spin-wave propagation in this plane (see Fig. 1). Then, in accordance with [1–4], the spin-wave frequency (1) acquires a shift, so that the modified dispersion relation reads

$$\omega(\mathbf{k}, \mathbf{E}) = \omega_0(\mathbf{k}) - \omega_E(\mathbf{k}). \quad (4)$$

Here $\omega_E(\mathbf{k}) = \omega_M \lambda_{SO} E a k_x$, $\omega_M = \gamma \mu_0 M_S$, $\lambda_{SO} = \frac{4A}{\mu_0 M_S^2} \frac{|e|}{a E_{SO}}$, a is a lattice parameter, and E_{SO} is an energy that is inverse proportional to the spin-orbit interaction strength (for YIG $E_{SO} = 3$ eV [2]). Note that the electric-field frequency shift—the last term of Eq. (4)—appears everywhere as an additive correction to the frequency ω in the spin-wave dispersion equation and can be taken into account simply by replacing ω by $\omega + \omega_E(\mathbf{k})$ in the zero-electric-field dispersion relation of a general form. Thus, the modified dispersion (4) is actually exact regardless of the approximations made and is independent of the order of the magnetostatic mode; for more details see Ref. [3].

One finds from Eq. (4) that not only the magnetodipolar coupling but also the external electric field generates in the $\omega(\mathbf{k})$ dependence a term linear in \mathbf{k} . However, there is an important difference in these terms. The electric-field contribution changes its sign with respect to the inversion of the wave vector \mathbf{k} or the electric-field direction, whereas the magnetodipolar (magnetostatic) contribution does not. Thus, the external electric field not only adds to the spin-wave frequency a contribution linearly dependent on the wave vector but also makes the spin-wave propagation nonreciprocal $\omega(\mathbf{k}, \mathbf{E}) \neq \omega(-\mathbf{k}, \mathbf{E})$. As shown in Fig. 2, one can tune the spin-wave dispersion by adjusting the electric field and thereby distinguish the electric-field effect from the magnetodipolar contribution unambiguously. For instance, under the influence of the external electric field, the spin-wave dispersion minimum is shifted from its position $f_{\min} = 7.72$ GHz at ($k_x = 0$, $k_y = 0$) in \mathbf{k} space and $E = 0$ down to $f_{\min} \approx 7.71$ GHz at $k_x \approx 3.75 \mu\text{m}^{-1}$ at $E = 30$ V/ μm (see Fig. 2). Numerical results given in Fig. 2 and the figures below are obtained for a thin film with interface-induced perpendicular magnetic anisotropy and material parameters: $M_S = 0.140$ MA/m, $K_U = -123$ J/m³, $A = 1.58$ pJ/m, $\mu_0 = 4\pi \times 10^{-7}$ H/m, $\gamma = 1.76 \times 10^{11}$ rad/(s T), and $\mu_0 H = 0.2$ T [3,20]; following Ref. [2], for parameter E_{SO} we took $E_{SO} = 3$ eV. We keep the film thickness fixed at $d = 10$ nm. Concerning the electric-field magnitude and experimental detection of the predicted

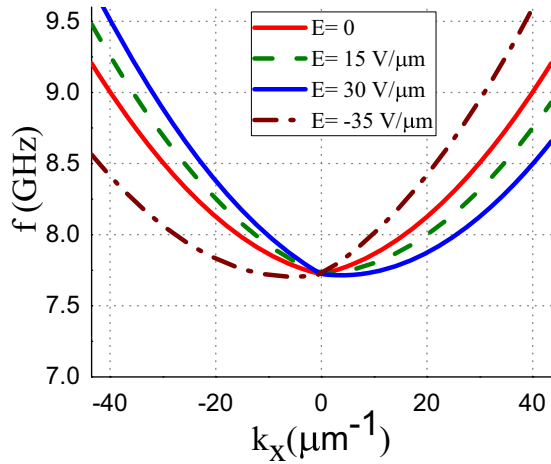


FIG. 2. The spin-waves dispersion in a thin ferromagnetic film, Eq. (4), taking into account the geometrical phase and the phase induced by the electric field $k_y = 0$. Along k_x axis the curves $f(\mathbf{k}, \mathbf{E})$ are symmetric. The spin-wave frequency minimum is at $k_x = 0.0$ at $E = 0$; $k_x \approx 7.77 \times 10^{-6} \mu\text{m}^{-1}$ at $E = 15 \text{ V}/\mu\text{m}$; $k_x \approx 3.75 \mu\text{m}^{-1}$ at $E = 30 \text{ V}/\mu\text{m}$; $k_x \approx -5.47 \mu\text{m}^{-1}$ at $E = -35 \text{ V}/\mu\text{m}$.

effects note that in the case of good quality magnetic film on a substrate, e.g., YIG on a gadolinium gallium garnet, the applied electric field can be quite large. In fact, we take into account already existing experimental [4,21,22] and theoretical reports [23] where an electric field of such magnitude is also discussed.

To understand how the electric field modifies the spin-wave dispersion, Fig. 3 presents the isofrequency contours $\omega(\mathbf{k}, \mathbf{E})$, Eq. (4), for E from 0 to 45 $\text{V}/\mu\text{m}$ with the frequency step $\Delta\omega/2\pi = \Delta f = 0.2 \text{ GHz}$. In zero electric field, the initial slope of the $\omega(\mathbf{k})$ depends on the angle between the wave vector \mathbf{k} and magnetization \mathbf{M}_S , as in Fig. 1. If this angle is smaller than the critical one, then the initial slope is negative [18]. The exchange contributes the term Dk^2 and for a short enough wavelength, the isofrequency contours form circles centered at the origin in k space, see Fig. 3(a). The external electric field pushes the isofrequency contours in the direction $(\mathbf{E} \times \mathbf{M}_S)$. Simultaneously, the spin-wave energy minimum is shifted down from its magnitude in the zero electric field. For example, the electric field of 45 $\text{V}/\mu\text{m}$, Fig. 3(d), shifts the energy minimum $f_{\min} \approx 7.72 \text{ GHz}$ at $(k_x = 0, k_y = 0)$ and $E = 0$ further to $(k_x \approx 8.94 \mu\text{m}^{-1}, k_y = 0)$ and now the lowest frequency is detected at $f_{\min} \approx 7.67 \text{ GHz}$ (see also related curves in Fig. 2). At some magnitude of the electric field E_c , $\omega(\mathbf{k}, E_c) = \omega_0(\mathbf{k}) - \omega_{E_c}(\mathbf{k}) = 0$ the frequency (4) equals zero at finite k_x . When the field is above the critical value $E > E_c$, the ferromagnetic state is unstable [1]. We will not discuss this case here.

Under the electric-field effect, in the low energy isofrequency curves a “dent” located along the $+k_x$ axis is rectified for $\mathbf{E} > 0$ (at $\mathbf{E} < 0$ a dent along the $-k_x$ axis is rectified), compare Figs. 3(e) and 3(f) for $E = +35$ and $-35 \text{ V}/\mu\text{m}$. The presence of a dent indicates that the curvature of the slowness curve changes sign. This means that the so-called caustics can be created. Caustics appear at points along the slowness curves at which its curvature goes to zero, resulting in a (formally) divergence in the power flow. Thus, in addition to the nonreciprocity, another remarkable feature of the electric-field

effect is the opportunity to generate focusing patterns from a single point source. We investigate this possibility in the next section.

III. SPIN-WAVE POWER FLOW

From Eq. (4) it is evident that the spin-wave dispersion is anisotropic, nonreciprocal, and depends on the in-plane wave vector direction with respect to the direction of $(\mathbf{E} \times \mathbf{M}_S)$ vector. These distinctive features modify the spin-wave propagation in a thin ferromagnetic film and lead to spin-wave power focusing beams—the caustics—appearing only on one side of the point source. As is known, the group velocity $\mathbf{v}_g = \partial\omega(\mathbf{k}, \mathbf{E})/\partial\mathbf{k}$ indicates the direction of the energy flow. In the case of Eq. (4) we have

$$\mathbf{v}_g = \partial\omega(\mathbf{k}, \mathbf{E})/\partial\mathbf{k} = \partial\omega_0(\mathbf{k})/\partial\mathbf{k} - \omega_M \lambda_{SO} E a \mathbf{e}_x. \quad (5)$$

Thus, a difference in the \mathbf{v}_g between the sides of the isofrequency curves at positive and negative values of k_x is simply proportional to the applied electric field. Equation (5) shows that we can realize the unidirectional caustic beams in the Damon-Eshbach geometry similar to those suggested in Ref. [13] but based on fundamentally different physics.

Figures 4(a)–4(e) illustrate schematically a general picture of the group velocity direction evolution in each point of $(\omega/2\pi, \mathbf{k})$ space as the field \mathbf{E} increases. As one can see, in general, at sufficiently small frequencies, the group velocity \mathbf{v}_g and the wave vector \mathbf{k} are noncollinear. This is a direct consequence of the anisotropy of the dispersion relation. Following Refs. [11,24,25], we call a spin-wave “forward” if $\mathbf{k}\mathbf{v}_g > 0$ and “backward” if $\mathbf{k}\mathbf{v}_g < 0$. With decreasing spin-wave wavelength, the exchange term Dk^2 becomes dominant and the isofrequency curves recover a more circular shape. Here we deal with the forward spin waves when the momentum and the energy propagation directions are parallel. Figures 4(e) and 4(f) illustrate how the spin-wave power flow direction can be manipulated by changing the electric-field sign.

The focusing of the magnetostatic surface and backward volume modes of dipolar and dipole-exchange waves in a ferromagnetic film was investigated in pioneering work [12]. In Ref. [13] the authors analyzed how the slowness surfaces change in thin ferromagnetic film with conventional DM interaction as the film thickness is increased and the magnetodipolar interaction becomes more important. We examine how the focusing effect can be manipulated by the external electric field keeping the YIG film thickness constant.

One of the requirements for waves caustic beam formation is that the group and phase velocities should point in different directions [11,25]. The focusing direction can be found from the isofrequency curve by traveling around the slowness surface and at each point calculating the normal to the surface. These normals indicate the directions of the energy flow. The amount of the energy sent in a given direction is proportional to the square root of the curvature of the slowness curve at that point. When the curvature is zero, one finds the caustics beams, when for waves with different wave vectors \mathbf{k} the group velocity \mathbf{v}_g is the same and, formally, in this direction the power flow diverges [11,12,25,26].

The overall picture of the group velocity patterns and appearance of the focusing beams are shown in Fig. 4. As

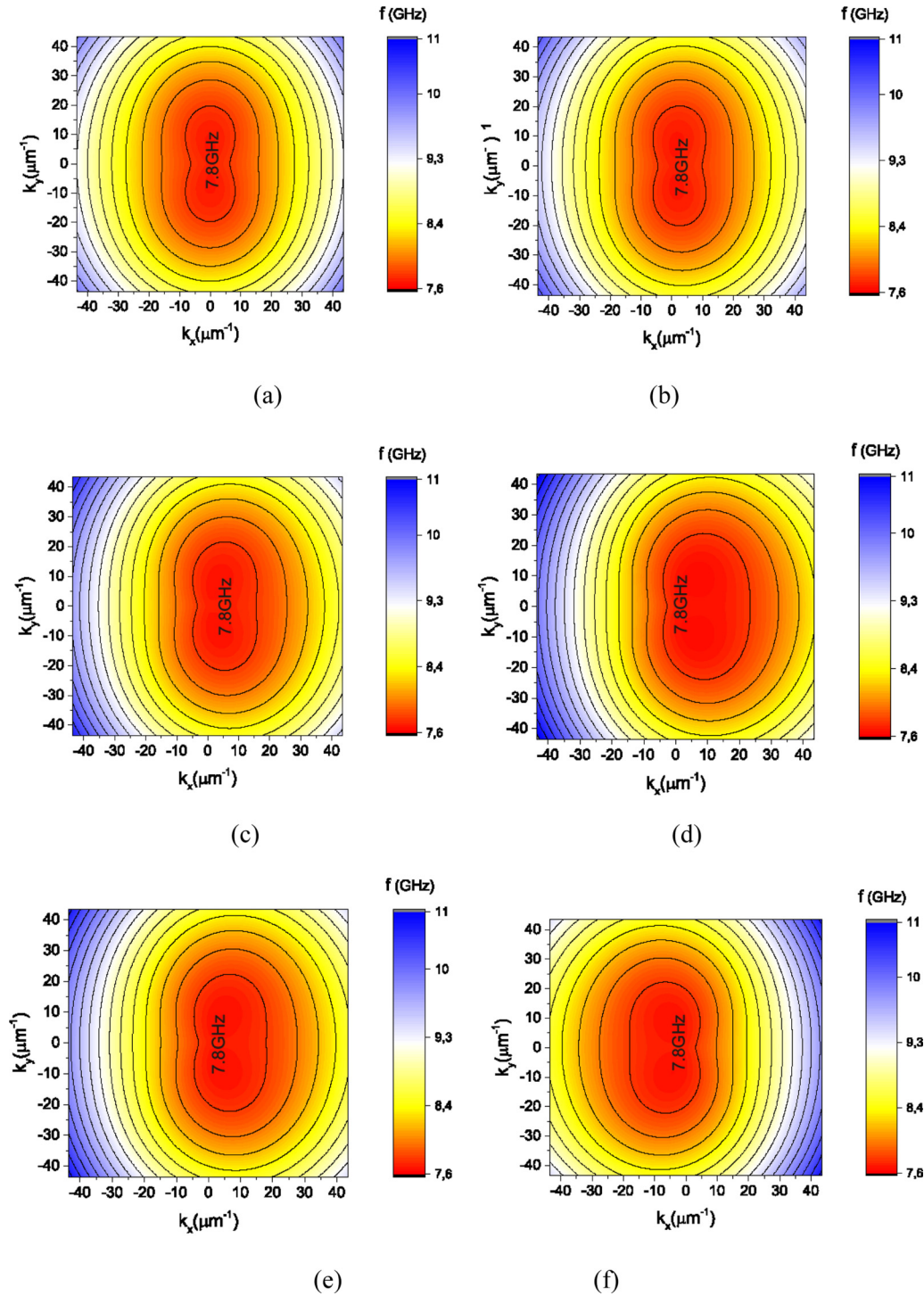


FIG. 3. Isofrequency contours of spin-wave dispersion relation Eq. (4) for E from 0 to $45 \text{ V}/\mu\text{m}$; the first isofrequency contour is at $f = 7.8 \text{ GHz}$; each successive contour represents a frequency difference $\Delta f = 0.2 \text{ GHz}$. (a) $E = 0$, (b) $E = 15 \text{ V}/\mu\text{m}$, (c) $E = 30 \text{ V}/\mu\text{m}$, (d) $E = 45 \text{ V}/\mu\text{m}$, (e) $E = +35 \text{ V}/\mu\text{m}$, and (f) $E = -35 \text{ V}/\mu\text{m}$.

one can see, already a weak electric field modifies the low energy isofrequency curves. The application of the external field leads to the curvature vanishing at two points along the slowness curve. This indicates that the curvature changes sign, which means that a caustic wave beam can form here. We illustrate this possibility in Fig. 5 where five different frequencies are shown for fixed $E = 10 \text{ V}/\mu\text{m}$, and in Fig. 6 where evolution of the slowness curve is shown for fixed

frequency $f = 8.2 \text{ GHz}$ under the effect of an external electric field. In the figures, the group velocity is indicated along each slowness curve (dashed lines with arrow). Solid (red) lines with arrow show the expected focusing directions (caustics). Formally, in this direction the power flow diverges [12,24,25]. Figures 6(e) and 6(f) illustrate how the spin-wave power flow direction can be manipulated by changing the electric-field sign.

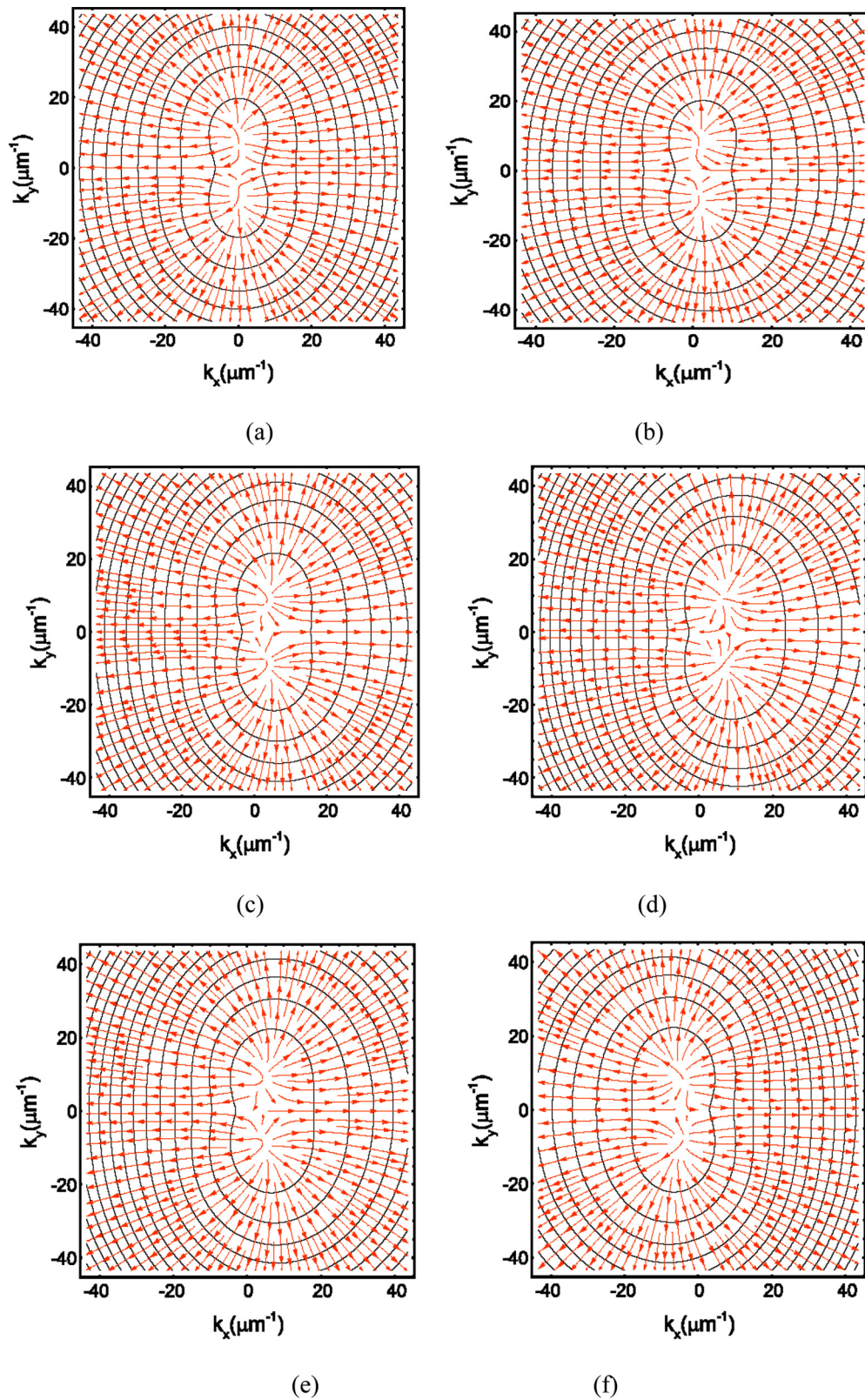


FIG. 4. The group velocity overall patterns. Here each contour in the figure represents a slowness surfaces and each successive contour represents a frequency difference $\Delta f = 0.2$ GHz; the first isofrequency contour is at $f = 7.8$ GHz. (a) $E = 0$, (b) $E = 15 \text{ V}/\mu\text{m}$, (c) $E = 30 \text{ V}/\mu\text{m}$, (d) $E = 45 \text{ V}/\mu\text{m}$, (e) $E = +35 \text{ V}/\mu\text{m}$, and (f) $E = -35 \text{ V}/\mu\text{m}$.

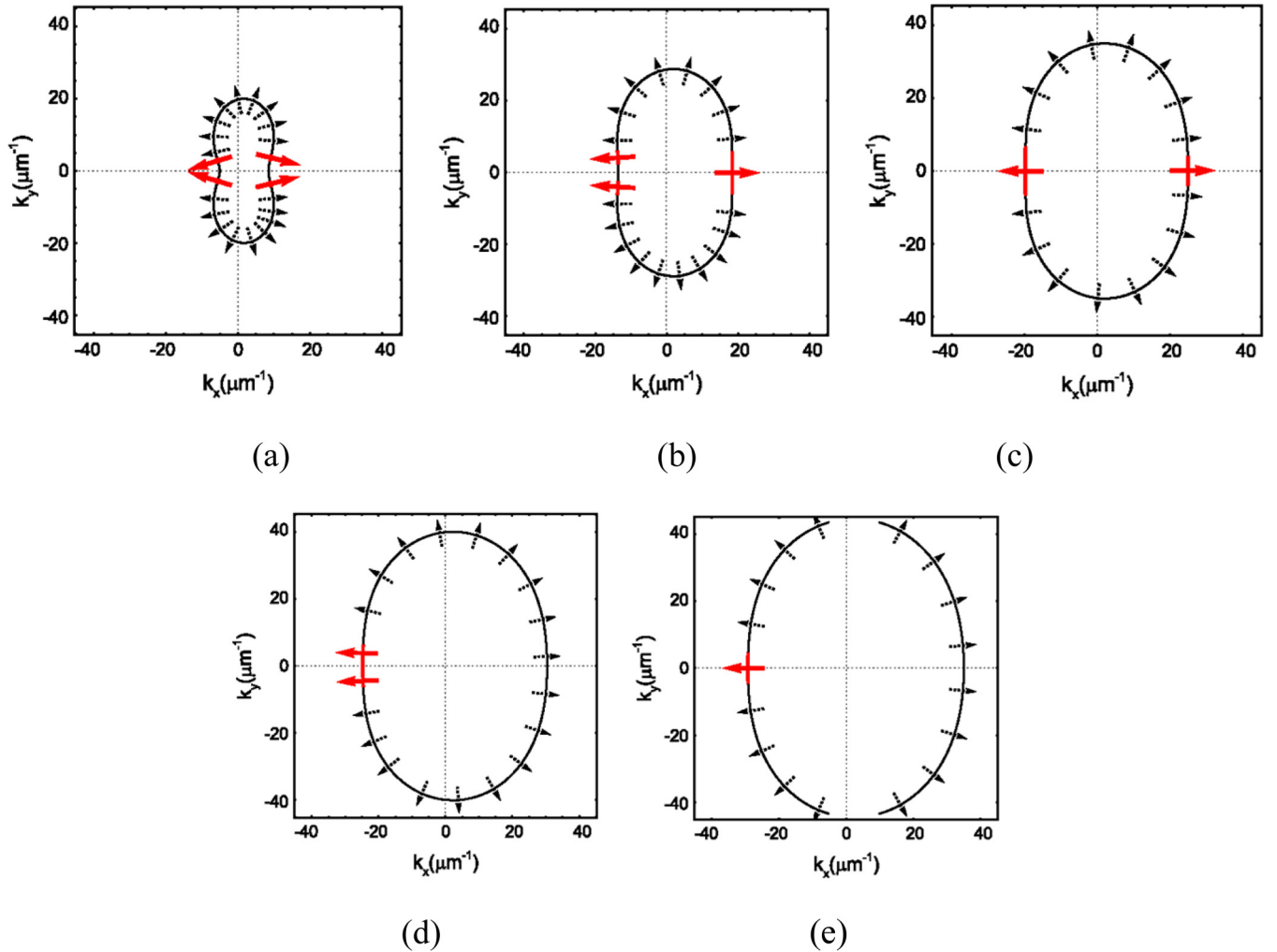


FIG. 5. Spin-wave focusing for different frequencies at a fixed electric field. Dashed lines with arrow denote the group velocity vectors \mathbf{v}_g directions. Long solid (red) lines with arrow represent focusing directions, or caustics, at given frequency. $E = 10$ V/ μm , $\mu_0 H = 0.2$ T. (a) $f = 7.8$ GHz, (b) $f = 8.0$ GHz, (c) $f = 8.2$ GHz, (d) $f = 8.4$ GHz, and (e) $f = 8.6$ GHz.

A C-shaped isofrequency contours mean another remarkable feature of the electric-field effect—an opportunity to generate *interference* patterns from a single point source. Evidence of the interference can already be seen in Fig. 5 for 7.8 and 8.0 GHz curves. As can be seen from the figure, these frequency contours demonstrate a C-shaped slowness curve. If we examine how the group velocity vector evolves around these curves, we notice that certain orientations of \mathbf{v}_g appear at multiple points along the curve. This indicates that propagation along these directions involves partial waves with different \mathbf{k} .

IV. CONCLUSION AND SUMMARY

Spin waves in some materials propagate a long distance with very little energy dissipation and therefore hold promise to substantially reduce the energy consumption in the next generation of electronic devices. One of primary goals of research in magnonics [27] is to find mechanisms that enable the electric-field control of spin dynamics since, in practice, an electric field is much easier to apply than a magnetic field.

As spins do not directly couple to the electric field, the electric-field control could be realized using various

magnetolectric effects. A few examples how the electric field can be used in the context of magnonics were recently demonstrated. The utilization of a magnetolectric film composite to control the phase of surface magnetostatic spin waves by a substrate strain induced electric field was demonstrated on the Ni/NiFe layers [28]. The feasibility of the electrical manipulation of spin-wave propagation in ultrathin Fe films through modulation of the exchange interaction by the electric field applied perpendicular to the magnetic film has been shown just recently in Ref. [29]. Of particular interest is also the effect of the voltage-controlled magnetic anisotropy, which manifests itself as a variation of the perpendicular magnetic anisotropy at the interface between a ferromagnetic metal and an insulator under the application of an interface voltage (see, e.g., [30,31] and references therein). Recent investigations in this field demonstrate that, due to spin-orbit coupling, there is a possibility to modify the spin-wave dispersion effectively [4] even in centrosymmetric magnets.

In this paper we have studied a power flow from a point source in thin magnetic films with induced DM-like interaction caused by an external electric field. Without an electric field, the power flow is essentially isotropic and energy radiates

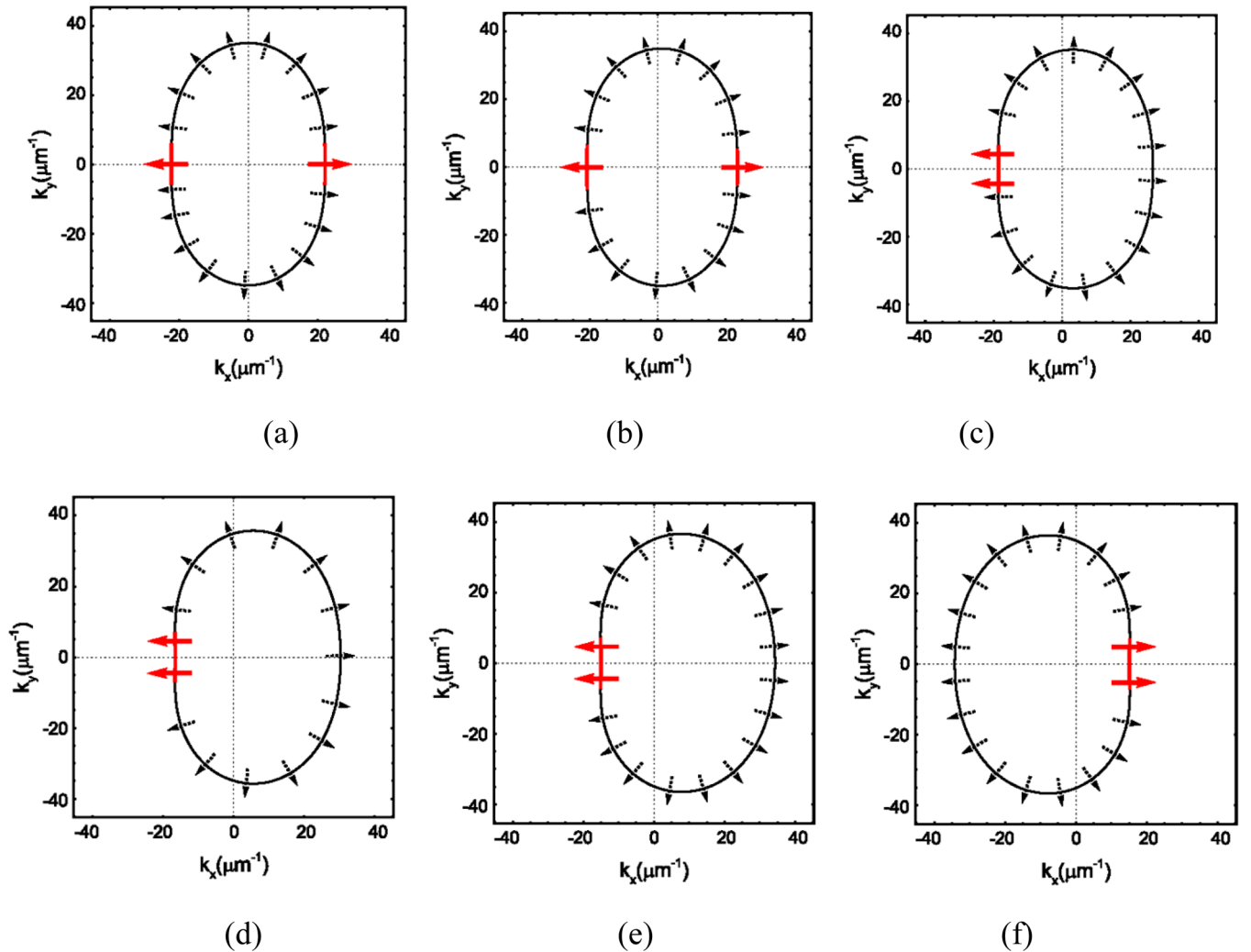


FIG. 6. Spin-wave focusing for fixed frequency under the effect of an external electric field. Dashed lines with arrow denote the group velocity vectors \mathbf{v}_g directions. Long solid (red) lines with arrow represent focusing directions (caustics). $f = 8.2$ GHz, $\mu_0 H = 0.2$ T. (a) $E = 0$, (b) $E = 5$ V/ μm , (c) $E = 15$ V/ μm , (d) $E = 25$ V/ μm , (e) $E = +35$ V/ μm , and (f) $E = -35$ V/ μm .

approximately equally in all directions. When the electric field is applied, we find a few remarkable results. Namely, by applying an electric field one can create caustics, highly focused beams of energy, at given frequencies. The focusing patterns are nonreciprocal, with the caustic beams appearing only on one side of a point source. There is also a possibility by inducing the DM-like interaction to create interference patterns. It was demonstrated that the degree of spin-wave power flow asymmetry can be effectively tuned with the external electric field. Thus, the external electric field gives a much more convenient opportunity to tune the dispersion relations and alter the focusing patterns in comparison with the film thickness changing. These effects have important implications for magnonic devices, where the transfer of angular momentum and energy play a key role. Thus, we have demonstrated that the electric field is an energy-efficient way to control the magnonic spin current propagating in insulating magnetic films.

Concerning an experimental detection of the predicted effects in practice, YIG with its uniquely low magnetic damping is a valuable material for these purposes [32]. Because the

exchange interaction governs the magnetic order in YIG and causes a large enough splitting between ferromagnetic (acoustic) and antiferromagnetic (optical) modes, one-sublattice ferromagnetic approximation for YIG is reasonable in a low-energy regime. In this case, the energy of acoustic magnons can be calculated within a conventional one-sublattice ferromagnetic approximation when all 20 magnetic moments in the primitive cell oscillate in phase and can be treated as one common magnetic moment. So, the results obtained here for a ferromagnet are applicable for YIG ferrimagnet directly.

ACKNOWLEDGMENTS

The authors are grateful for the valuable discussions with J. W. Klos and A. N. Kuchko. This research was conducted in the framework of the MagIC Project: 644348-H2020-MSCA-RISE-2014; V.N.K. and A.S.S. also acknowledge support of the State Fund for Fundamental Research of Ukraine (Project: F71/59-2017).

- [1] D. L. Mills and I. E. Dzyaloshinskii, *Phys. Rev. B* **78**, 184422 (2008).
- [2] T. Liu and G. Vignale, *Phys. Rev. Lett.* **106**, 247203 (2011).
- [3] T. Liu and G. Vignale, *J. Appl. Phys.* **111**, 083907 (2012).
- [4] X. Zhang, T. Liu, M. E. Flatté, and H. X. Tang, *Phys. Rev. Lett.* **113**, 037202 (2014).
- [5] Y. Aharonov and A. Casher, *Phys. Rev. Lett.* **53**, 319 (1984).
- [6] Z. Cao, X. Yu, and R. Han, *Phys. Rev. B* **56**, 5077 (1997).
- [7] C. S. Davies, A. Francis, A. V. Sadovnikov, S. V. Chertopalov, M. T. Bryan, S. V. Grishin, D. A. Allwood, Y. P. Sharaevskii, S. A. Nikitov, and V. V. Kruglyak, *Phys. Rev. B* **92**, 020408(R) (2015).
- [8] C. S. Davies and V. V. Kruglyak, *Low Temp. Phys.* **41**, 760 (2015).
- [9] X. Xing and Y. Zhou, *NPG Asia Mater.* **8**, e246 (2016).
- [10] M. Jamali, J. H. Kwon, S.-M. Seo, K.-J. Lee, and H. Yang, *Sci. Rep.* **3**, 3160 (2013).
- [11] A. V. Vashkovsky and E. H. Lock, *Phys. Usp.* **49**, 389 (2006).
- [12] V. Veerakumar and R. E. Camley, *Phys. Rev. B* **74**, 214401 (2006).
- [13] J.-V. Kim, R. L. Stamps, and R. E. Camley, *Phys. Rev. Lett.* **117**, 197204 (2016).
- [14] C. W. Sandweg, Y. Kajiwara, A. V. Chumak, A. A. Serga, V. I. Vasyuchka, M. B. Jungfleisch, E. Saitoh, and B. Hillebrands, *Phys. Rev. Lett.* **106**, 216601 (2011).
- [15] J. Fernández-Rossier, M. Braun, A. S. Núñez, and A. H. MacDonald, *Phys. Rev. B* **69**, 174412 (2004).
- [16] B. A. Kalinikos, *IEEE Proc.* **127**, 4 (1980).
- [17] B. A. Kalinikos and A. N. Slavin, *J. Phys. C: Solid State Phys.* **19**, 7013 (1986).
- [18] R. P. Erickson and D. L. Mills, *Phys. Rev. B* **46**, 861 (1992).
- [19] R. Arias and D. L. Mills, *Phys. Rev. B* **60**, 7395 (1999).
- [20] S. Lee, S. Grudichak, J. Sklenar, C. C. Tsai, M. Jang, Q. Yang, H. Zhang, and J. B. Ketterson, *J. Appl. Phys.* **120**, 033905 (2016).
- [21] G. Schileo, C. Pascual-Gonzalez, M. Alguero, I. M. Reaney, P. Postolache, L. Mitoseriu, K. Reichmann, and A. Feteira, *J. Am. Ceram. Soc.* **99**, 1609 (2016).
- [22] S. Takano, E. Kita, K. Siratori, K. Kohn, S. Kimura, and A. Tasaki, *Ferroelectrics* **161**, 73 (1994).
- [23] V. Petrov, M. Bichurin, A. Saplev, A. Tatarenko, and V. Lobekin, *J. Appl. Phys.* **121**, 224103 (2017).
- [24] E. H. Lock, *Phys. Usp.* **51**, 375 (2008).
- [25] A. V. Vashkovsky and E. H. Lock, *Phys. Usp.* **54**, 281 (2011).
- [26] T. Schneider, A. A. Serga, A. V. Chumak, C. W. Sandweg, S. Trudel, S. Wolff, M. P. Kostylev, V. S. Tiberkevich, A. N. Slavin, and B. Hillebrands, *Phys. Rev. Lett.* **104**, 197203 (2010).
- [27] V. V. Kruglyak, S. O. Demokritov, and D. Gründler, *J. Phys. D: Appl. Phys.* **43**, 264001 (2010).
- [28] M. Bao, G. Zhu, K. L. Wong, J. L. Hockel, M. Lewis, J. Zhao, T. Wu, P. K. Amiri, and K. L. Wang, *Appl. Phys. Lett.* **101**, 022409 (2012).
- [29] S. Wang, X. Guan, X. Cheng, C. Lian, T. Huang, and X. Miao, *Sci. Rep.* **6**, 31783 (2016).
- [30] R. Verba, M. Carpentieri, G. Finocchio, V. Tiberkevich, and A. Slavin, *Sci. Rep.* **6**, 25018 (2016).
- [31] Qi Wang, A. V. Chumak, L. Jin, H. Zhang, B. Hillebrands, and Zh. Zhong, *Phys. Rev. B* **95**, 134433 (2017).
- [32] A. A. Serga, A. V. Chumak, and B. Hillebrands, *J. Phys. D: Appl. Phys.* **43**, 264002 (2010).